RESEARCH ARTICLE

Decolorization of methylene blue by silver/reduced graphene oxide-ethylene diamine nanomaterial: synthesis, characterization, and optimization

Ümit Ecer[1] · Aybek Yiğit[2] · Nurettin Menges[3] · Tekin Şahan[4]

Abstract

In this study, ethylene diamine-coated reduced graphene oxide-supported silver composite (Ag/rGO-ED) was synthesized and used as an efficient catalyst for the decolorization of methylene blue (MB) in the presence of $NaBH_4$. The morphology of the obtained material was elucidated using field emission scanning electron microscopy (FE-SEM), Fourier-transform infrared spectroscopy (FTIR), energy-dispersive X-ray analysis (EDX), transmission electron microscopy (TEM), and X-ray diffraction (XRD) techniques. The influences of four parameters (MB concentration (mg/L), $NaBH_4$ amount (mM), catalyst amount (g/L), and contact time (s)) on the decolorization process were appraised and optimized via response surface methodology (RSM). For the decolorization of MB, the optimum solutions were obtained as C_o of 32.49 mg/L, $NaBH_4$ amount of 152.89 mM, catalyst amount of 0.83 g/L, and 101.39 s contact time with MB decolorization efficiency of 97.73%. MB, a pollutant in wastewater, was decolorized rapidly by Ag/rGO-ED with an efficiency of approximately 97%. The exploration of kinetics and thermodynamics was another major emphasis of the work. The activation energy (E_a) and rate constant (k) for the decolorization of MB were obtained as 37.9 kJ/mol and 0.0135 s^{-1}, respectively. The obtained results show that the catalyst, a new composite material in the literature, is promising for decolorization of wastewater.

Introduction

In the last century, soil, air, and water have been significantly polluted by the growing population. Therefore, it is important extremely that water resources are clean and wastewater should be reused. Wastewater containing pollutants (dyes, heavy metals, etc.) from textile, paper, chemical, food, and cosmetics industries cause environmental pollution (Ahmadipour et al. 2020). Dye molecules are undesirable in wastewater, even in small amounts, because they color the water, give it an unesthetic appearance, and disrupt aquatic life processes. Most dyes are not biodegradable and block light from entering the water and photosynthesis. Some dyes are toxic to living organisms and sometimes even carcinogenic and mutagenic, so they must be carefully removed (Huang et al. 2019). Methylene blue (MB) is a cationic dye, used widely for dying wool, cotton, and silk. The presence of MB in wastewater poses risks to human life, such as nausea, diarrhea, and vomiting (El-Sharkawy et al. 2007). In order to eliminate this problem, it is important to treat wastewater containing dyes by providing more and better alternatives, and many studies are being carried out in this regard (Ali 2010; Antony et al. 2023, Ecer and Yılmaz 2024). Extensive approaches such as ion exchange (Joseph et al. 2020), membrane filtration (Rashidi et al. 2015), flocculation/coagulation (Sadri Moghaddam et al. 2010), adsorption (Ecer et al. 2021), reverse osmosis (Al-Bastaki 2004), and degradation/

✉ Ümit Ecer
umitecer@gmail.com

1 Department of Chemical Engineering, Institute of Natural and Applied Sciences, Van Yuzuncu Yil University, 65080 Van, Turkey

2 The Research Laboratory Application and Research Center, Igdir University, Igdir, Turkey

3 Department of Biomedical Engineering, Faculty of Engineering, Necmettin Erbakan University, 42100 Konya, Turkey

4 Department of Chemistry, Faculty of Science, Van Yuzuncu Yil University, 65080 Van, Turkey

decolorization (Ecer and Yılmaz 2024) are used for the remediation of dye-contaminated wastewater.

The decolorization procedure with NaBH4 present is a useful method for removing dyestuff. A reducing substance, $NaBH_4$, can be applied to dyes to catalytically decolorize them, especially if metal nanoparticles are present. The surfaces of the catalyst play a significant role in the transfer of H_2 from $NaBH_4$ to pollutant molecules by electron transfer. Processes for decolorization of pollutants using metallic catalysts are comparable to other processes in terms of activity and efficiency as they have similar application methods. Catalyst/NaBH4 processes provide advantages such as not creating waste sludge compared to other removal techniques. Catalysts can be reused and can be utilized in a higher pH range (Ecer and Yılmaz 2024, Naz et al. 2021).

Recently, the application of metal nanoparticles has been examined in the field of catalysis. Interesting catalytic activity was shown for some areas such as organic reactions and dye decolorization. Noble metal nanoparticles (silver, palladium, platinum, gold, etc.) have attracted great attention due to their unique physical, chemical, and biological properties in many fields for chemical, catalytic, and environmental applications (Antony et al. 2023, Kora and Rastogi 2016, Wadhwani et al. 2018). When it comes to metal nanoparticles, support materials are essential, especially for catalysis and other industrial uses. Support materials play a crucial role in stabilizing, dispersing, and augmenting the catalytic characteristics of metal nanoparticles, rendering them more robust and efficient for a range of applications such as sensing, nanotechnology, and catalysis. With advances in materials science, new carbon-based nanoparticles such as CNTs, graphene oxide, and graphene are being developed (Pyrzynska 2011; Yang et al. 2011). Some advantages that come with the nano-sized structures are high adsorption capacity, quick equilibrium rates, and efficacy across a broad pH range (Mauter and Elimelech 2008). Among the nanostructures reported in the literature, graphene's planar structure and enormous surface area (2630 m^2/g for single-layer graphene) are thought to make it an effective adsorbent. The removal of organic contaminants and dyes from industrial wastes has attracted a lot of interest to graphene oxide (GO) recently, including graphene nanocomposites, chemically functionalized graphene, and reduced graphene oxide (rGO) (Chowdhury and Balasubramanian 2014, Yusuf et al. 2015). According to research, GO and its biopolymer composites work well as adsorbents to remove organic dyes (Fan et al. 2013; Liu et al. 2012; Ramesha et al. 2011).

Effective optimization techniques can be applied to further enhance the decolorization process. The traditional method of studying decolorization depends on varying one parameter while maintaining the same values for the other parameters. Consequently, the traditional approach necessitates time, effort, and chemical use to examine every parameter.

Response surface methodology (RSM), an optimization technique, is a collection of statistical and mathematical methodologies used to create an experimental methodology for creating and refining the modeling of processes. RSM makes it possible to see how a set of controlled variables that have an impact on the independent variable relate to it (Ecer and Yılmaz 2024, Hai et al. 2023, Weremfo et al. 2023).

Several composite materials have been employed in the literature to reduce or eliminate dye pollution from aqueous media. Nevertheless, there is not much research about the synthesis, characterization, design, and use of materials as a catalyst for the decolorization/degradation of dye molecules. In this study, to decolorize methylene blue dye, a new catalyst including Ag NPs was synthesized supported on ethylene diamine-coated reduced graphene oxide (Ag/rGO-ED). By employing the synthesized composite material, the current work seeks to close a research gap and further understanding of the decolorization of dyes like MB. The synthesized catalyst was thoroughly examined utilizing a variety of characterization methods. The effect of several parameters was investigated by applying RSM for optimization of the decolorization process. In conclusion, the optimization method offers a fresh approach to wastewater treatment for both the efficient utilization of catalysts and the catalytic reduction of dyes. Considering all these, it is estimated that the study will make a significant contribution to the literature and can be a reference for future studies.

Materials and methods

Material and instrumentations

Graphite, thionyl chloride ($SOCl_2$), dimethylformamide (DMF), potassium permanganate ($KMnO_4$), anhydrous tetrahydrofuran (THF), hydrazine hydrate (NH_2NH_2), ethylenediamine, sodium nitrate, sodium borohydride ($NaBH_4$), sulfuric acid (H_2SO_4), silver nitrate ($AgNO_3$), hydrogen peroxide (H_2O_2), and methylene blue ($C_{16}H_{18}ClN_3S \cdot 3H_2O$) were all analytical quality reagents received from Sigma-Aldrich (Germany). Dye concentrations before and after decolorization were determined by UV–Vis spectrophotometer (Thermo Scientific, Genesys 10S, USA). The prepared nanoparticles were characterized using different techniques. The surface structure and morphology of each sample were characterized by Field emission scanning electron microscopy (FE-SEM) (Zeiss ZEISS GeminiSEM 500 and Hitachi Regulus 8230 FE-SEM instrument with X1000 magnification and 10 kV voltage). To ascertain morphological alterations, the Hitachi HT7800 type transmission electron microscopy (TEM) apparatus was employed. Imaging was done with a voltage of 100 kV and a magnification of 70000X. Fourier transform infrared (FTIR) spectra was recorded by using Nicolet S10

spectrometric analyzer in the 500–4000 cm^{-1} region (Thermo Scientific, USA). The X-ray diffraction (XRD) pattern of the nanoparticles was obtained employing a Panalytical EMPY-REAN diffractometer between 2Θ = 10–80°.

Catalyst synthesis

Synthesis of GO

Marcano and colleagues presented a straightforward modification to the Hummers method for synthesizing GO, which was obtained from graphite powder (Köktürk et al. 2022; Marcano et al. 2010; Yardım et al. 2017). In a nutshell, concentrated H$_2$SO$_4$ (115 mL) was combined with 5.0 g of graphite flakes and 2.5 g of NaNO$_3$ in a 2000-mL glass conical flask, and the mixture was chilled to 0 °C. Next, KMnO$_4$ (15.0 g) was gradually added to the medium, while the mixture was vigorously stirred in the magnetic stirrer. After heating the mixture to 35 °C, it was stirred for 40–45 min. Then, in order to prevent a significant exothermic reaction up to 98 °C, 230 mL of water was gradually added to the mixture. To fully oxidize the graphite, the suspension was maintained at this temperature for 15 min at a different temperature. Following a 10-min cooling period in a water bath, 600 mL of water was added to dilute the suspension, and 5 mL of 30% H$_2$O$_2$ was added as well. The resultant suspension was filtered, cleaned with 5% HCl and water, and then dried to produce graphite oxide once it cooled to room temperature.

Synthesis of rGO nanoparticles

The Hummers method was used to prepare GO. rGO was prepared by sonicating 100 mg of GO in 50 mL of pure water within a 500-mL conical flask for a predetermined amount of time. Following some mixing, 17 mL of NH$_2$NH$_2$ and 200 mL of DMF were added to the reaction media. To ensure that the graphite oxide formed r-GO, it was agitated at 90 °C for 24 h before being cooled to room temperature (Imer et al. 2020; Marcano et al. 2010; Safari et al. 2016).

Synthesis of rGO-ED nanoparticles

In this step, the synthesis of the particles was done in three steps. The first stage involved adding 10 mL SOCl$_2$ and 1 mL DMF to a 50-mL glass flask containing 100 mg rGO. The flask was then spun in a magnetic stirrer at low temperature for a full day. After a full day, the resultant mixture was removed and cleaned using THF filtration. After that, it was dried at low temperature in an oven. The second phase involved adding 3 mL of ethylene diamine to a 25-mL glass flask containing the 100 mg of rGO-Cl that had been obtained in the previous step. The combination was then agitated at 116 °C for a whole day. Following filtration, THF was used to wash the resultant mixture. After that, it was dried at low temperature in an oven (Köktürk et al. 2022) (Fig. 1).
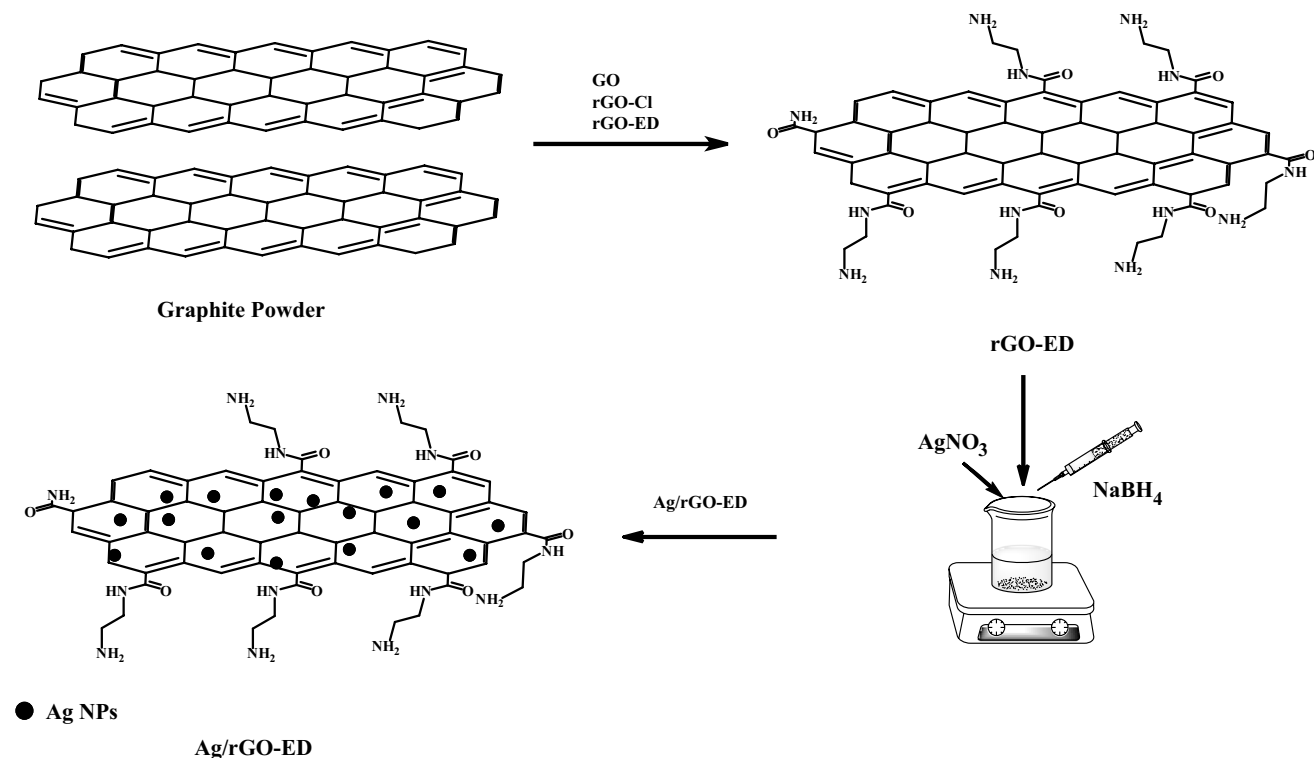

Fig. 1 Schematic illustration of synthesis Ag/rGO-ED nanoparticles

Synthesis of Ag/rGO-ED nanoparticles

The NaBH$_4$ reduction procedure was used to synthesize the Ag(0)-doped catalyst. Ag(0) loading was planned to be 10% w/t based on the support material. First, a certain quantity of rGO-ED was dissolved in purified water to create the Ag/rGO-ED. The required quantity of AgNO$_3$ was then added, and the mixture was agitated for a whole day. After that, the solution was vigorously stirred, while the necessary quantity of NaBH$_4$ was added to convert Ag(I) to Ag(0). It was centrifuged and dried at 60 °C for 2 h.

Decolorization of MB and optimization

The decolorization of MB was investigated using Ag/rGO-ED in the presence of NaBH$_4$. All the catalytic tests were carried out in a flask in which the volume of the solution was 5 mL. Decolorization efficiency (%) was obtained under varied conditions including MB concentration (Co, mg/L), NaBH$_4$ amount (mM), catalyst amount (g/L), and contact time (s). The experimental conditions for the decolorization process are given in Table 1. The of MB concentration was determined at 664 nm using UV–Vis spectroscopy (Fig. 2). The decolorization (%) is calculated from Eq. 1:

Table 1 RSM-CCD matrix for decolorization of MB

Parameters	Code	Level and range (coded)		
		-1	0	1
Initial conc. (mg/L)	X_1	10	30	50
NaBH$_4$ amount (mM)	X_2	50	150	250
Catalyst amount (g/L)	X_3	0.1	0.55	1
Contact time (sec.)	X_4	10	80	150
Run	X_1	X_2	X_3	X_4	% Decolorization

Run	X_1	X_2	X_3	X_4	% Decolorization
1	30.00	50.00	0.55	80.00	85.07
2	50.00	250.00	0.10	10.00	76.48
3	30.00	150.00	0.55	10.00	87.50
4	10.00	50.00	1.00	150.00	85.30
5	30.00	150.00	0.55	80.00	97.63
6	30.00	150.00	0.55	80.00	98.54
7	50.00	50.00	0.10	150.00	83.29
8	10.00	50.00	0.10	10.00	62.81
9	30.00	150.00	0.55	80.00	97.88
10	50.00	50.00	1.00	10.00	85.04
11	50.00	250.00	1.00	10.00	84.60
12	30.00	150.00	0.55	80.00	98.80
13	30.00	150.00	1.00	80.00	95.83
14	10.00	250.00	0.10	150.00	82.20
15	50.00	150.00	0.55	80.00	91.54
16	30.00	250.00	0.55	80.00	87.91
17	10.00	50.00	0.10	150.00	81.50
18	50.00	250.00	0.10	150.00	83.24
19	50.00	250.00	1.00	150.00	84.21
20	30.00	150.00	0.55	80.00	98.86
21	10.00	250.00	0.10	10.00	74.50
22	10.00	250.00	1.00	10.00	83.21
23	50.00	50.00	0.10	10.00	71.32
24	30.00	150.00	0.55	150.00	93.83
25	50.00	50.00	1.00	150.00	84.90
26	30.00	150.00	0.10	80.00	87.50
27	10.00	50.00	1.00	10.00	75.60
28	30.00	150.00	0.55	80.00	97.96
29	10.00	150.00	0.55	80.00	88.80
30	10.00	250.00	1.00	150.00	84.80

$$Decolorization\% = \frac{(C_o - C_e)}{C_o} \times 100 \qquad (1)$$

where C_o and C_e are initial and equilibrium MB concentrations, respectively.

Decolorization was investigated using three-level central composite design (CCD) with four parameters. The process parameters of X_1, C_o; X_2, NaBH$_4$ amount; X_3, catalyst amount; and X_4, contact time were examined to optimize the decolorization process (Table 1). The interaction of independent variables and response can be represented mathematically as given below (Eq. 2):

$$y_p = \beta_o + \sum_{i=1}^{k} \beta_i x_i + \sum_{i=1}^{k} \beta_{ii} x_i^2 + \sum_{i=1}^{k} \sum_{j=i+1}^{k} \beta_{ij} x_i x_j \qquad (2)$$

where y_p is the response, x_i and x_j are the independent variables and β_0 is constant, β_i is linear, β_{ii} is square, and β_{ij} is interaction effect of the model. Analysis of variance (ANOVA) was used to verify the statistical significance and applicability of the proposed model. The correlation coefficient (R^2), Fisher value (F value), and probability value (p value) were examined to explain the substantial contribution of each parameter and fit of the proposed model.

Results and discussion

Catalyst characterizations

The morphology of rGO-ED and Ag/rGO-ED nanoparticles were observed by FE-SEM, and the images are shown in Fig. 3. For imaging morphological changes that happen on the surface, a FE-SEM instrument is recommended. Layers that are irregular in surface shape, randomly folded, and folded over one another are notable in the images of rGO-ED (a) (Al-Qadri et al. 2022; Tawade et al. 2020). The mass percentages of C, N, and O in the study using FESEM-EDX (a) were found to be 63.37, 19.92, and 16.71%, respectively. A ZEISS GeminiSEM 500 type FE-SEM instrument was used for characterizations, with X10000 magnification and 2 kV voltage. The FE-SEM (b) images of silver modification on rGO-ED show that the transparent Ag (silver) surface has been altered. In addition, the examination of rGO-ED-Ag with the FESEM-EDX (b) detector revealed 15.6% Ag (Moazami et al. 2016) (Fig. 3).

The morphology and size of rGO-ED nanoparticles were studied using TEM. Particle morphological, structural, and dimensional analysis is possible with TEM equipment. The imaging process yielded average particle size of 7.3835 ± 1.7773 (min–max, 5.142–11.058) nm for rGO-ED. Furthermore, the histograms of particle size for roughly 15 randomly chosen particles are provided below (Fig. 4) (Aygün et al. 2020; Yigit et al. 2021).

FTIR analysis of rGO-Cl and rGO-ED given in Fig. 5. Based on the obtained spectrum, the vibration bands identified as -OH and NH groups were found between 3000 and 3500 cm^{-1}, C-H groups were found between 2500 and 3000 cm^{-1}, C=O' groups were found between 1500 and 2000 cm^{-1}, and C=C groups were matched with C-H groups at 1000–1500 cm^{-1}. Additionally, the C-N and N–H groups matched the 1000–1500 cm^{-1} vibration bands (Vijina et al. 2023, Irani et al. 2018) (Fig. 5).

The crystal structures of the materials were obtained by XRD for rGO, rGO-CI, and rGO-ED (Fig. 6). The ideal tool for determining the size, orientation, and crystallographic structure of solid materials is the XRD instrument. GO is responsible for the diffraction peaks in the spectrum at $2\theta = 10.81°$ and $2\theta = 43.28°$, while rGO is responsible for the peak at $2\theta = 26.02°$. Nonetheless, it may be claimed that in experimental investigations, acylation (rGO-Cl) caused the peak to somewhat enlarge. The diffraction peak at $2\theta = 18.52°$, and the peaks at $2\theta = 19.00°$ and $2\theta = 21.06°$ (rGO-ED) can be matched after amine group alteration (Fig. 6). This was reported by Samadaei et al. (2015), Sadhukhan et al. (2016), Maharana et al. (2017), Vinodh et al. (2019), and Köktürk et al. (2022).

CCD model analysis

Experimental conditions for the decolorization of MB by Ag/rGO-ED were optimized using CCD-RSM. Four factors (initial concentration, NaBH$_4$ amount, catalyst amount, and contact time) with important effects on the decolorization performance of Ag/rGO-ED were selected as factors for CCD design based on the conclusions of the experiments. Table 1 lists the tests that were performed and the outcomes that were attained.

The main purpose was to provide a trustworthy regression model that simulated the decolorization of MB in wastewater by varying parameters. After the investigation, the following quadratic polynomial regression equation was obtained for the decolorization efficiency of MB concerning the independent variables:

$$\begin{aligned}
\%Decolarization =\ & +40.22778 + 0.76869[Initial\ Conc.] + 0.27440[NaBH_4\ amount] \\
& +27.54844[Catalyst\ amount] + 0.24756\ [Time] - 0.000485[Initial\ Conc.][NaBH_4\ amount] \\
& -0.024167[Initial\ Conc.][Catalyst\ amount] - 0.000869643[Initial\ Conc.][Time] \\
& -0.016056[NaBH_4\ amount][Catalyst\ amount] - 0.000219643[NaBH_4 amount][Time] \\
& -0.068254[Catalyst\ amount][Time] - 0.000901893[Initial\ Conc.]^2 - 0.00072922[NaBH_4\ amount]^2 \\
& -10.42430[Catalyst\ amount]^2 - 0.000634882[Time]^2
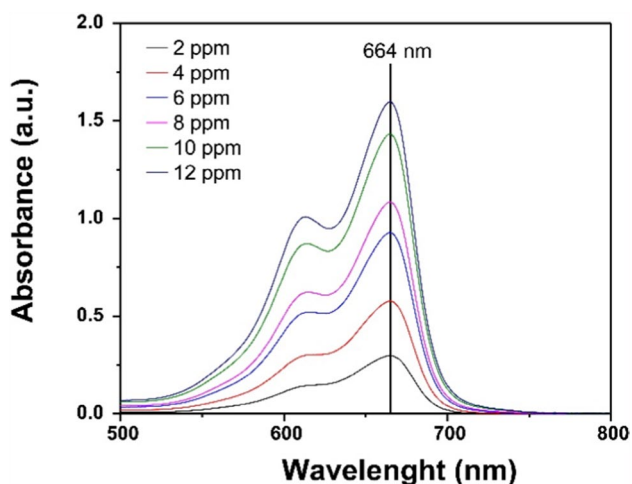\end{aligned} \qquad (3)$$

Fig. 2 UV–vis spectrum for MB

To evaluate the correctness of the resulting model, analysis of variance (ANOVA) was utilized to generate all statistical controls (adjusted R^2, R^2, F value, p value, and lack of fit). The conclusions are given in Table 2. The significance of the model is suggested by its F value of 25.24. A large "Model F-value" like this is 0.01% likely to be the result of noise. "Prob > F" values less than 0.0500 suggest the significance of the model terms (Malla et al. 2023; Sadri Moghaddam et al. 2010). Important model terms in this case are A, B, C, D, BD, CD, A^2, and B^2. When the values exceed 0.1000, it means that the model terms are not significant. The R^2 and *Adj R^2* of the model were obtained as 0.9593 and 0.9213, indicating that the data fit very well with the selected model.

A diagnostic plot of the predicted and actual values is shown in Fig. 7a. The outcome demonstrates that the predicted and actual values agree. This suggests that the obtained model is accurate and that there was only minor model violation. Furthermore, all of the points that correspond to yield are randomly distributed and located within boundaries close to the zero axis in the range between ± 3.0, as seen from the plot of the internally studentized residuals against the predicted values in Fig. 7b. Because the residuals and actual values are so close to one another, the model does
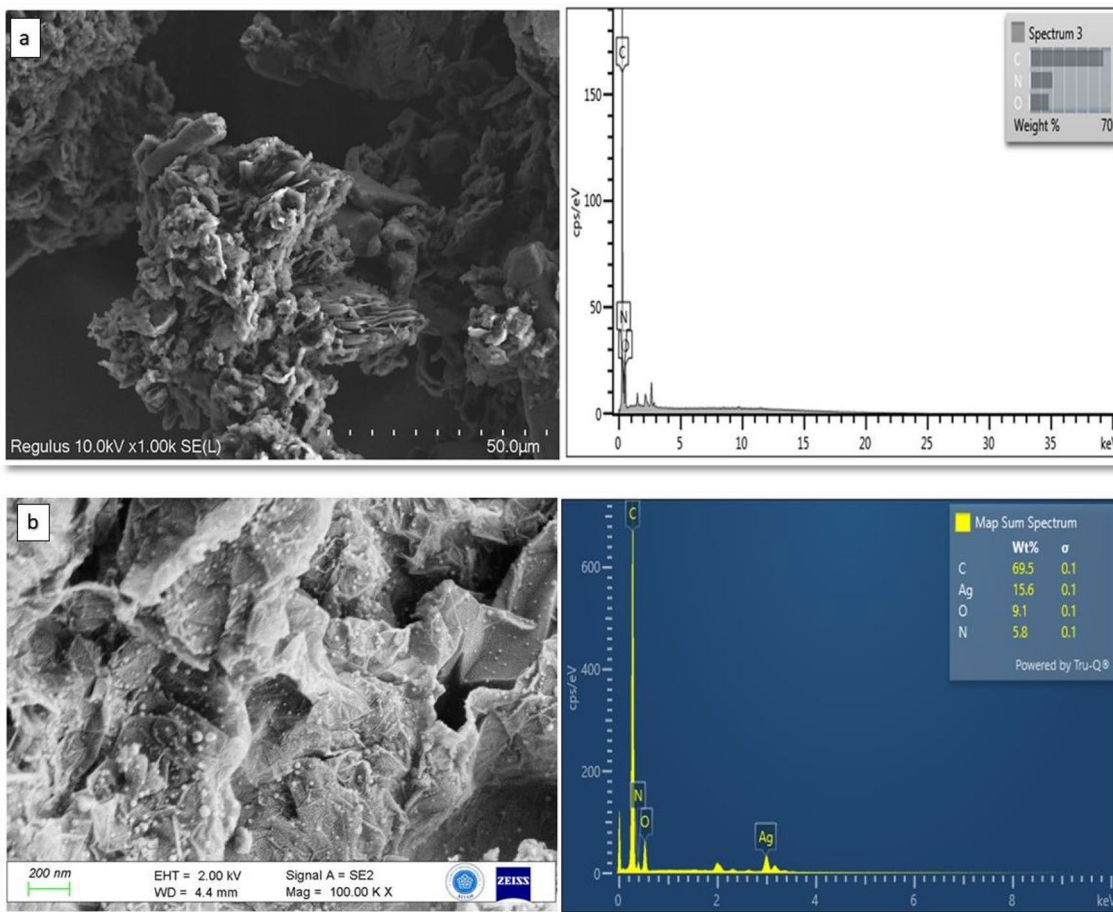

Fig. 3 FE-SEM images of **a** rGO-ED and **b** Ag/rGO-ED nanoparticles

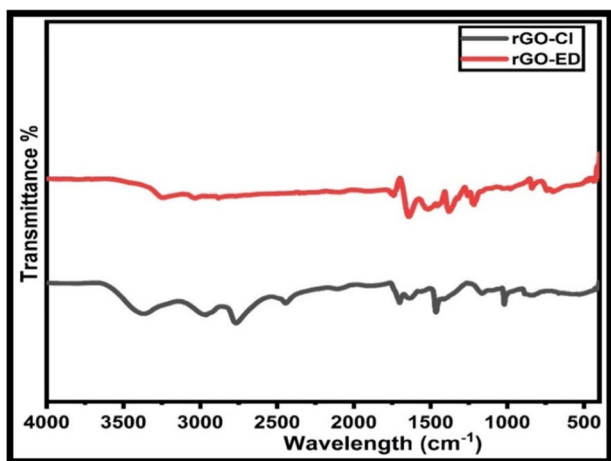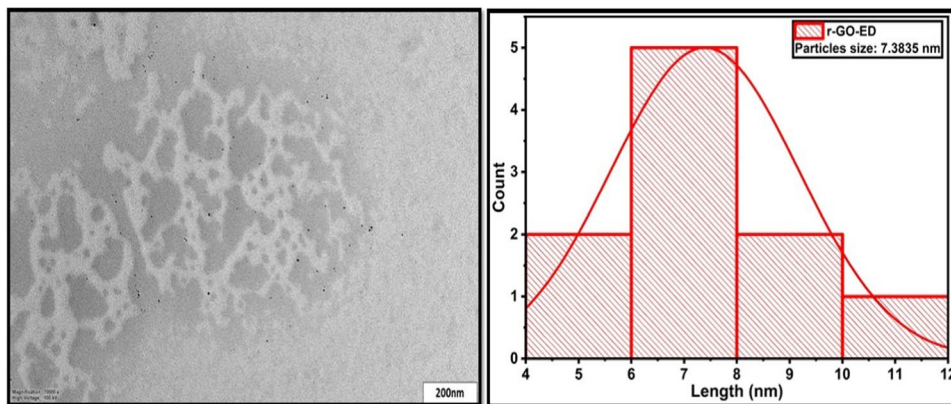**Fig. 4** TEM images and histogram distribution plot of rGO-ED nanoparticles

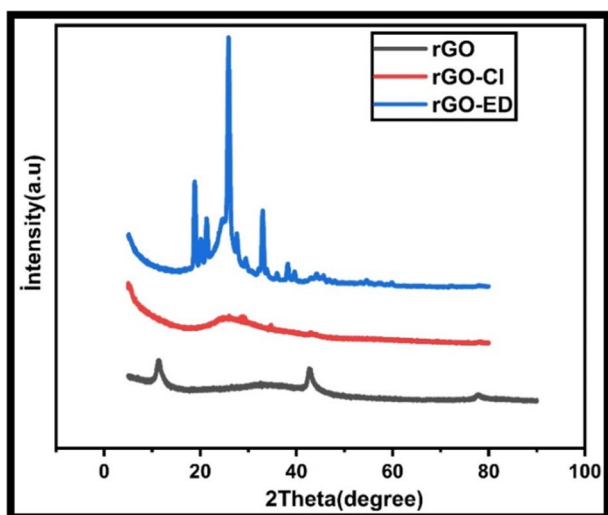**Fig. 5** FT-IR spectra for the rGO-Cl and rGO-ED

Fig. 6 XRD patterns of rGO, rGO-Cl, and rGO-ED nanoparticles

a good job of capturing the relationship between yield and process parameters (Elganidi et al. 2022; Kumar et al. 2018).

3D plots produced by CCD-RSM were used to reveal the effects of the independent parameters and to determine the optimal conditions for maximum response. To shed light on the role of $NaBH_4$ in the decolorization of MB, the effect of the $NaBH_4$ was examined. The obtained findings are shown in Fig. 8a. An increase in $NaBH_4$ concentration initially caused greater decolorization. This increases the amount of hydrogen and electrons produced, which may help transfer them to MB molecules through Ag NPs and accelerate the catalytic reduction of MB. During the catalytic reduction, MB molecules and BH_4^- firstly diffuse from the aqueous solution to the catalyst surface. Then, to speed up electron transfer from BH_4^- to MB, Ag NPs on the surface function as an electron relay system (Ecer and Yılmaz 2024). One could say that the concentration of $NaBH_4$ reaches peak effectiveness at roughly 150 mM. Nevertheless, a negative impact on the catalytic reduction of MB was observed when the fixed amount of Ag/rGO-ED resulted in increased $NaBH_4$. This is because there is more $NaBH_4$ present and more hydrogen is adsorbed onto the catalyst surface as a result. The decrease in the decolorization of MB is understood when one considers that both the amount of catalyst and Ag are constant (Li et al. 2019). To examine the impact of reaction time on the decolorization process, experiments were conducted within the time interval of 10–150 s. Over time, the efficiency of MB decolorization increased and seemed to peak at around 100 s (Fig. 8a).

The initial MB concentration range of 10–50 mg/L was investigated to examine the impact of the Ag-doped catalyst. Firstly, the decolorization of MB rises with increasing concentration as seen in Fig. 8b. A significant portion of MB is reduced quickly due to the decolorization process being initially rapid. The Ag/rGO-ED surface has enough active sites to sufficiently the cope with the rise in concentration, which might be the cause of this increase. The decolorization efficiency appears to decrease after a certain point. The amount of MB that can be reduced is constrained because

Table 2 ANOVA of quadratic model for the decolorization (%) of MB

Source	Sum of squares	df	Mean square	F value	p Value Prob > F	
Model	2167,639	14	154.8314	25.24443	< 0.0001	significant
Initial conc. (mg/L), X_1	37.26722	1	37.26722	6.076223	0.0263	
NaBH$_4$ amount (mM), X_2	38.4661	1	38.4661	6.271693	0.0243	
Catalyst amount (g/L), X_3	204.379	1	204.379	33.32292	< 0.0001	
Contact time (sec.), X_4	215.3041	1	215.3041	35.10419	< 0.0001	
$X_1 X_2$	15.0544	1	15.0544	2.45454	0.1380	
$X_1 X_3$	0.7569	1	0.7569	0.123409	0.7303	
$X_1 X_4$	23.7169	1	23.7169	3.866915	0.0680	
$X_2 X_3$	8.3521	1	8.3521	1.361766	0.2614	
$X_2 X_4$	37.8225	1	37.8225	6.166758	0.0253	
$X_3 X_4$	73.96	1	73.96	12.05878	0.0034	
X_1^2	33.71955	1	33.71955	5.497793	0.0332	
X_2^2	137.851	1	137.851	22.47587	0.0003	
X_3^2	11.54505	1	11.54505	1.882359	0.1902	
X_4^2	25.07436	1	25.07436	4.088242	0.0614	

$R^2 = 0.9593$, $Adj\ R^2 = 0.9213$

Fig. 7 Diagnostic plots for decolorization efficiency, **a** predicted versus actual values and **b** studentized residuals versus predicted values
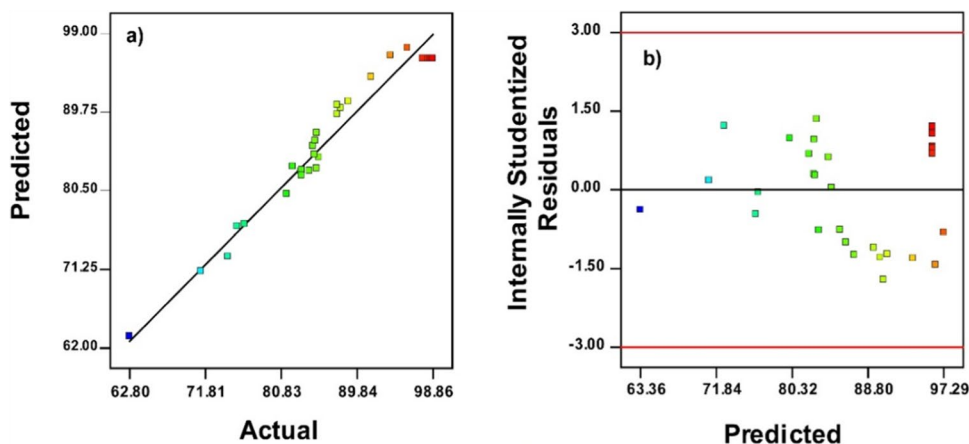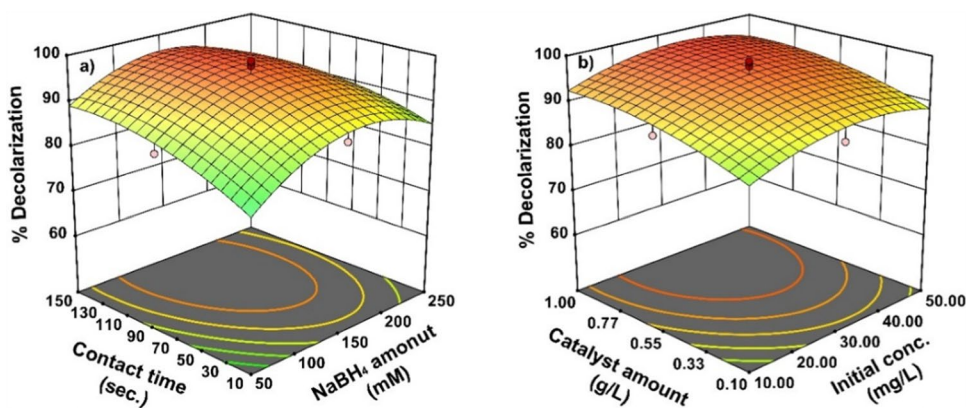

Fig. 8 3D graphs for the decolorization of MB as a function of **a** time-NaBH$_4$ and **b** initial concentration-catalyst amount

there is a constant quantity of catalyst and NaBH$_4$ in the solution. For this reason, it is natural for decolorization to decrease as the concentration of MB increases (Ecer and Yılmaz 2024, Li et al. 2019). Also, Fig. 8b shows the results

of the decolorization process regarding the Ag/rGO-ED amount. The efficiency of decolorization rose as the catalyst concentration rose to approximately 0.55 g/L. Efficiency increases in tandem with this because there are more active

sites due to the increased amount of catalyst. The increase in Ag/rGO-ED led to the creation of more catalytic active sites and reactive surfaces for MB molecules, which accelerated the transport of electrons and reactive hydrogens to the target pollutant. Further increasing the amount of catalyst resulted in decreasing efficiency. Later, the decrease in yield can be explained by the fact that suspended particles rise more when the Ag/rGO-ED amount increases (Daneshvar et al. 2003). As a result, there were fewer active sites, which in turn caused the yield to drop.

The essential objective of this study was to figure out the optimal conditions for maximum decolorization efficiency by Ag/rGO-ED. The optimal values for process variables and response were selected following the experimental and numerical optimization. The optimal response was defined by a quadratic model including the process variables. Four process parameters of initial concentration, NaBH$_4$ amount, catalyst amount, and time were investigated to achieve the maximum decolorization %. The optimal solutions selected for the decolorization % are base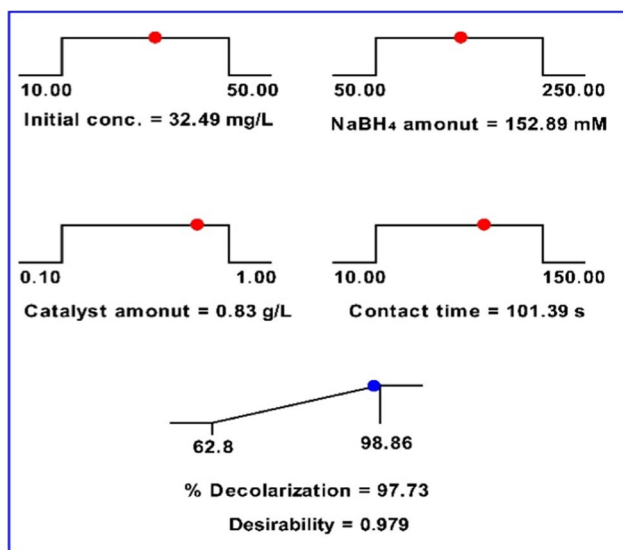d on an initial MB concentration of 32.49 mg/L, NaBH$_4$ amount of 152.89 mM, catalyst amount of 0.83 g/L, and 101.39 s of contact time. Under these conditions, the efficiency was determined as 97.73%. The determined ranges and optimum values of decolorization results are given in Fig. 9. In the verification experiments carried out under these conditions, the result was confirmed to be 98%, compatible with the numerical optimization result.

Table 3 compares the catalytic activity of the Ag/rGO-ED catalyst, which was utilized for the decolorization of MB, with other catalysts found in the literature. Compared to different catalyst systems reported in the literature for MB decolorization, the catalyst produced seems to exhibit higher or comparable catalytic activity. Furthermore, the optimization procedure for the efficient use of catalysts as well as the catalytic reduction of dyes in the current work presents a novel viewpoint on wastewater treatment. Taking all of these into account, it is projected that the study will significantly add to the body of literature and serve as a resource for further research.

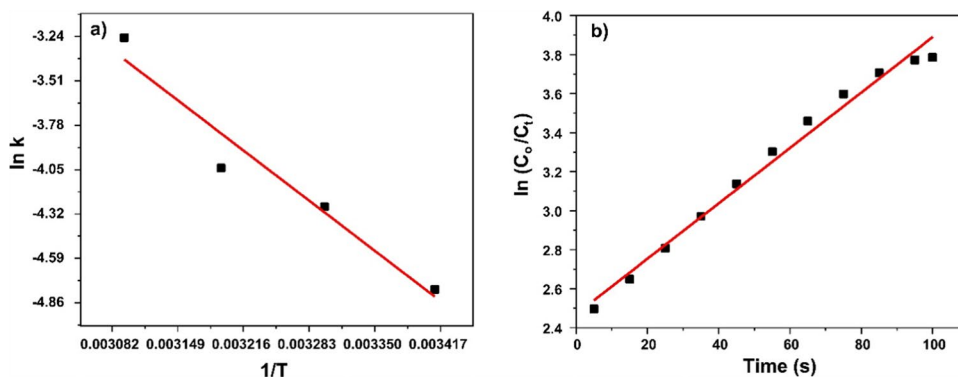## Thermodynamic and kinetic analyses for decolorization of MB

Under the determined optimum conditions, the effect of temperature on the decolorization of MB was investigated. The effectiveness of MB decolorization was positively impacted by temperature increases. The Arrhenius equation (Eq. 4) was used to determine the apparent activation energy (E$_a$) for decolorization of MB by Ag/rGO-ED based on the kinetic rate constant (k) at various temperatures (25–50 °C).

$$\ln k = -\frac{E_a}{RT} + \ln A \tag{4}$$

where E$_a$ (J/mol) is the apparent activation energy; A is the pre-exponential factor; T (K) is the absolute temperature; and R (8.314 J/mol K) is the ideal gas constant. The plot of ln k versus 1/T is given in Fig. 10a. E$_a$ was calculated as 37.9 kJ/mol.

Furthermore, at the optimal conditions identified, the pseudo-first-order (PFO) kinetic equation derived from experimental

Fig. 9 Desirability ramps for optimization criteria

Table 3 Comparison of several catalysts for MB decolorization

Catalyst	Reaction conditions	Decolorization efficiency	Ref
Ag/rGO-ED	32.49 mg/L MB, 152.89 mM NaBH$_4$, 0.83 g/L catalyst	97.7% for 101.39 s	This study
NiO NPs	50 mM NaBH$_4$, 50 ppm MB, 10 mg catalyst	98% for 13 min	(Baytar et al. 2023)
Ag-PDA-MS	40 mg/L MB, 0.1 M NaBH$_4$	99.4% for 1 min	(Tan 2024)
ZBD@Ag	35.7 mM NaBH$_4$, 0.05 mM MB, 0.2 mg/mL catalyst	99% for 6 min	(Lajevardi et al. 2019)
Au@TA-GH	10 mg/L MB, 2 mg catalyst	~ 100% for 9 min	(Luo et al. 2015)
Cotton@Ag NPs	50 mg catalyst, 50 mg/L MB, 0.02 M NaBH$_4$	>99% for 8 min	(Qi et al. 2020)
CuNPs-templated CS nanocatalyst	0.31 mM MB, 1.2 g/L catalyst, 0.5 M NaBH$_4$	>98% for 7 min	(Godiya et al. 2023)

Fig. 10 **a** lnk versus 1/T and **b** ln(C_o/C_t) versus t plots for decolorization of MB

data was employed to enhance comprehension of the mechanism involved in the decolorization process. The decolorization efficiency increased with longer contact time. The PFO model and the obtained response agreed rather well. The relationship between the response time and ln C_t/C_o was linear.

$$\ln \left(C_t/C_o \right) = -kt \tag{5}$$

where C_o and C_t are at the initial and at time t concentration (mg/L), k (min^{-1}) is the rate constant, and t is the contact time (min.). The linear plot of ln (C_o/C_t) versus t is given in Fig. 10b. k was obtained as 0.0135 s^{-1} for the decolorization process of MB by Ag/rGO-ED.

Possible decolorization mechanism of MB

The possible decolorization mechanism of MB with NaBH4 in the presence of Ag/rGO-ED is described in Fig. 11. The catalytic reduction of MB by Ag/rGO-ED composites can be explained by the electron transfer effect. Ag NPs can transport

electrons between donors and receptors and are strong conductors. Consequently, Ag NPs mediate this catalytic activity via the redox mechanism, allowing electrons to move from the donor (BH_4^-) to the acceptor (MB) (Baytar et al. 2023; Patel et al. 2022). Here, firstly, MB and $NaBH_4$ adsorb on the catalyst surface. Electrons can then be transferred from BH_4^- to MB with the help of the Ag-doped catalyst, resulting in the decolorization of MB to leuco-methylene blue (Abay et al. 2017). Finally, leuco-methylene blue spontaneously desorbs from the Ag/rGO-ED surface and diffuses into the solution due to the weaker electrostatic effect between the catalyst and leuco-methylene blue. As a result, MB, which has harmful effects on the environment, turns into leuco-methylene blue, a colorless and non-peaking form (Sankaran et al. 2021).

Conclusion

Consequently, a highly efficient hybrid catalyst, Ag/rGO-ED, was produced with a cheap and simple synthetic technique and had excellent dye decolorization capabilities in the
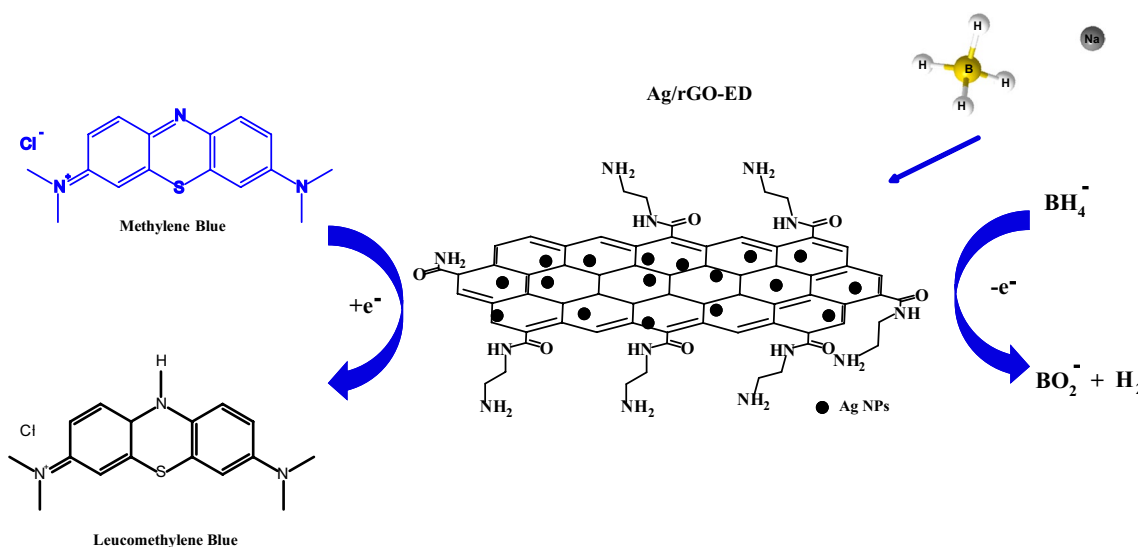

Fig. 11 Possible decolorization mechanism for MB by Ag/rGO-ED

presence of NaBH$_4$. The morphology and structure of the catalyst were characterized using different techniques. Ag/rGO-ED nanoparticles were used to decolorize MB in the presence of NaBH4, and CCD-RSM was utilized to optimize the variables. The generated model was effective in predicting the decolorization of MB dye, as demonstrated by the statistical significance of the *p* value, *F* value, and R^2 for the proposed model, according to the ANOVA findings. Another key focus of the work was the investigation of thermodynamics and kinetics. The maximum decolorization efficiency was achieved at 97.73% under optimum Co 32.49 mg/L, NaBH$_4$ amount 152.89 mM, catalyst amount 0.83 g/L, and 101.39 s contact time. The degradation of MB by Ag/rGO-ED yielded an apparent activation energy (Ea) of 37.9 kJ/mol and a rate constant (k) of 0.0135 s^{-1}. Additionally, the catalytic activity of Ag/rGO-ED was compared with various catalysts in the literature. It is believed that the efficient decolorization of MB by Ag/rGO-ED will pave the way for more research on the decolorization/degradation of other dyes.

Author contribution Ü.E.: investigation, data analysis, material synthesis, and characterization, writing-reviewing and editing. A.Y.: data analysis, experiments, methodology, material synthesis and characterization, writing and reviewing. N.M.: data analysis, methodology, characterization, writing, and reviewing. T.Ş.: investigation, material synthesis, characterization, writing and reviewing.

Data Availability The authors confirm that the data supporting the findings of this study are available within the article.

Declarations

Ethics approval The authors all agree to ethical approval and understand its related rules and content.

Consent to participate The authors of this manuscript are all aware of the journal to which the manuscript was submitted, and all agree to continue to support the follow-up work.

Consent for publication This manuscript has not been submitted or published in other journals, and the authors agree to consent to publish.

Competing interests The authors declare no competing interests.

References

Abay AK, Chen X, Kuo D-H (2017) Highly efficient noble metal free copper nickel oxysulfide nanoparticles for catalytic reduction of 4-nitrophenol, methyl blue, and rhodamine-B organic pollutants. New J Chem 41:5628–5638. https://doi.org/10.1039/C7NJ00676D

Ahmadipour M, Arjmand M, Thirmizir MZA, Le AT, Chiam SL, Pung S-Y (2020) Synthesis of core/shell-structured CaCu$_3$Ti$_4$O$_{12}$/SiO$_2$ composites for effective degradation of rhodamine B under ultraviolet light. J Mater Sci: Mater Electron 31:19587–19598. https://doi.org/10.1007/s10854-020-04486-1

Al-Bastaki N (2004) Removal of methyl orange dye and Na$_2$SO$_4$ salt from synthetic waste water using reverse osmosis. Chem Eng Process 43:1561–1567. https://doi.org/10.1016/j.cep.2004.03.001

Ali H (2010) Biodegradation of synthetic dyes—a review. Water Air Soil Pollut 213:251–273. https://doi.org/10.1007/s11270-010-0382-4

Al-Qadri AAQ, Drmosh QA, Onaizi SA (2022) Enhancement of bisphenol a removal from wastewater via the covalent functionalization of graphene oxide with short amine molecules. Case Stud Chem Environ Eng 6:100233. https://doi.org/10.1016/j.cscee.2022.100233

Antony AM, Yelamaggad CV, Patil SA (2023) Palladium nanoparticles decorated on functionalized graphitic carbon nitride as an efficient and retrievable nanocatalyst for organic dye degradation and hydrogen peroxide sensing. Mater Chem Phys 297:127370. https://doi.org/10.1016/j.matchemphys.2023.127370

Aygün A, Gülbağça F, Nas MS, Alma MH, Çalımlı MH, Ustaoglu B, Altunoglu YC, Baloğlu MC, Cellat K, Şen F (2020) Biological synthesis of silver nanoparticles using Rheum ribes and evaluation of their anticarcinogenic and antimicrobial potential: A novel approach in phytonanotechnology. J Pharm Biomed Anal 179:113012. https://doi.org/10.1016/j.jpba.2019.113012

Baytar O, Ekinci A, Şahin Ö, Kutluay S (2023) Green synthesis of NiO from watermelon seed shell extract for the evaluation of H2 production from NaBH4 hydrolysis and photocatalytic reduction of methylene blue. Mater Sci Eng: B 296:116704. https://doi.org/10.1016/j.mseb.2023.116704

Chowdhury S, Balasubramanian R (2014) Recent advances in the use of graphene-family nanoadsorbents for removal of toxic pollutants from wastewater. Adv Coll Interface Sci 204:35–56. https://doi.org/10.1016/j.cis.2013.12.005

Daneshvar N, Salari D, Khataee AR (2003) Photocatalytic degradation of azo dye acid red 14 in water: investigation of the effect of operational parameters. J Photochem Photobiol: A Chem 157:111–116. https://doi.org/10.1016/S1010-6030(03)00015-7

Ecer Ü, Yılmaz Ş (2024) Fabrication of magnetic biochar-MIL-68(Fe)-supported cobalt composite material toward the catalytic reduction performance of crystal violet. Jo Water Process Eng 57:104574. https://doi.org/10.1016/j.jwpe.2023.104574

Ecer Ü, Zengin A, Şahan T (2021) Magnetic clay\zeolitic imidazole framework nanocomposite (ZIF-8@Fe$_3$O$_4$@BNT) for reactive orange 16 removal from liquid media. Colloids Surf: A Physicochem Eng Asp 630:127558. https://doi.org/10.1016/j.colsurfa.2021.127558

Elganidi I, Elarbe B, Ridzuan N, Abdullah N (2022) Optimisation of reaction parameters for a novel polymeric additives as flow improvers of crude oil using response surface methodology. J Pet Explor Prod Technol 12:437–449. https://doi.org/10.1007/s13202-021-01349-1

El-Sharkawy EA, Soliman AY, Al-Amer KM (2007) Comparative study for the removal of methylene blue via adsorption and photocatalytic degradation. J Colloid Interface Sci 310:498–508. https://doi.org/10.1016/j.jcis.2007.02.013

Fan L, Luo C, Sun M, Qiu H, Li X (2013) Synthesis of magnetic β-cyclodextrin–chitosan/graphene oxide as nanoadsorbent and its application in dye adsorption and removal. Colloids Surf: B Biointerfaces 103:601–607. https://doi.org/10.1016/j.colsurfb.2012.11.023

Godiya CB, Kumar S, Park BJ (2023) Superior catalytic reduction of methylene blue and 4-nitrophenol by copper nanoparticles-templated chitosan nanocatalyst. Carbohydr Polym Technol Appl 5:100267. https://doi.org/10.1016/j.carpta.2022.100267

Hai ND, Dat NM, Nam NTH, An H, Tai LT, Cong CQ, Huong QTT, Hieu NH (2023) Phytosynthesis of silver nanoparticles@graphene oxide using Mangifera indica leaves extract at room temperature: the simultaneous effects of synthesis conditions on controlled

particle size and colorimetric sensing of H2O2. Diam Relat Mater 138:110264. https://doi.org/10.1016/j.diamond.2023.110264

Huang T, Yan M, He K, Huang Z, Zeng G, Chen A, Peng M, Li H, Yuan L, Chen G (2019) Efficient removal of methylene blue from aqueous solutions using magnetic graphene oxide modified zeolite. J Colloid Interface Sci 543:43–51. https://doi.org/10.1016/j.jcis.2019.02.030

Imer AG, Gülcan M, Çelebi M, Tombak A, Ocak YS (2020) Effects of the r-GO doping on the structural, optical and electrical properties of CdO nanostructured films by ultrasonic spray pyrolysis. J Mater Sci: Mater Electron 31:2111–2121. https://doi.org/10.1007/s10854-019-02732-9

Irani V, Tavasoli A, Vahidi M (2018) Preparation of amine functionalized reduced graphene oxide/methyl diethanolamine nanofluid and its application for improving the CO2 and H2S absorption. J Colloid Interface Sci 527:57–67. https://doi.org/10.1016/j.jcis.2018.05.018

Joseph J, Radhakrishnan RC, Johnson JK, Joy SP, Thomas J (2020) Ion-exchange mediated removal of cationic dye-stuffs from water using ammonium phosphomolybdate. Mater Chem Phys 242:122488. https://doi.org/10.1016/j.matchemphys.2019.122488

Köktürk M, Yildirim S, Yiğit A, Ozhan G, Bolat İ, Alma MH, Menges N, Alak G, Atamanalp M (2022) What is the eco-toxicological level and effects of graphene oxide-boramidic acid (GO-ED-BA NP) ?: In vivo study on Zebrafish embryo/larvae. J Environ Chem Eng 10:108443. https://doi.org/10.1016/j.jece.2022.108443

Kora AJ, Rastogi L (2016) Catalytic degradation of anthropogenic dye pollutants using palladium nanoparticles synthesized by gum olibanum, a glucuronoarabinogalactan biopolymer. Ind Crops Prod 81:1–10. https://doi.org/10.1016/j.indcrop.2015.11.055

Kumar S, Jain S, Kumar H (2018) Performance evaluation of adaptive neuro-fuzzy inference system and response surface methodology in modeling biodiesel synthesis from jatropha–algae oil. Energy Sources, Part A: Recover Util Environ Eff 40:3000–3008. https://doi.org/10.1080/15567036.2018.1515277

Lajevardi A, Tavakkoli Yaraki M, Masjedi A, Nouri A, Hossaini Sadr M (2019) Green synthesis of MOF@Ag nanocomposites for catalytic reduction of methylene blue. J Mol Liq 276:371–378. https://doi.org/10.1016/j.molliq.2018.12.002

Li Y, Lu H, Wang Y, Li X (2019) Deposition of Au nanoparticles on PDA-functionalized PVA beads as a recyclable catalyst for degradation of organic pollutants with NaBH4 in aqueous solution. J Alloy Compd 793:115–126. https://doi.org/10.1016/j.jallcom.2019.04.148

Liu F, Chung S, Oh G, Seo TS (2012) Three-dimensional graphene oxide nanostructure for fast and efficient water-soluble dye removal. ACS Appl Mater Interfaces 4:922–927. https://doi.org/10.1021/am201590z

Luo J, Zhang N, Lai J, Liu R, Liu X (2015) Tannic acid functionalized graphene hydrogel for entrapping gold nanoparticles with high catalytic performance toward dye reduction. J Hazard Mater 300:615–623. https://doi.org/10.1016/j.jhazmat.2015.07.079

Maharana HS, Rai PK, Basu A (2017) Surface-mechanical and electrical properties of pulse electrodeposited Cu–graphene oxide composite coating for electrical contacts. J Mater Sci 52:1089–1105. https://doi.org/10.1007/s10853-016-0405-7

Malla MA, Dubey A, Kumar A, Yadav S, Kumari S (2023) Modeling and optimization of chlorpyrifos and glyphosate biodegradation using RSM and ANN: elucidating their degradation pathways by GC-MS based metabolomics. Ecotoxicol Environ Saf 252:114628. https://doi.org/10.1016/j.ecoenv.2023.114628

Marcano DC, Kosynkin DV, Berlin JM, Sinitskii A, Sun Z, Slesarev A, Alemany LB, Lu W, Tour JM (2010) Improved synthesis of graphene oxide. ACS Nano 4:4806–4814. https://doi.org/10.1021/nn1006368

Mauter MS, Elimelech M (2008) Environmental applications of carbon-based nanomaterials. Environ Sci Technol 42:5843–5859. https://doi.org/10.1021/es8006904

Moazami A, Montazer M, Dolatabadi MK (2016) Tunable functional properties on polyester fabric using simultaneous green reduction of graphene oxide and silver nitrate. Fibers Polym 17:1359–1370. https://doi.org/10.1007/s12221-016-6597-2

Naz M, Rafiq A, Ikram M, Haider A, Ahmad SOA, Haider J, Naz S (2021) Elimination of dyes by catalytic reduction in the absence of light: a review. J Mater Sci 56:15572–15608. https://doi.org/10.1007/s10853-021-06279-1

Patel P, Maliekal PJ, Lingayat S, Badani PM (2022) Understanding the kinetics and reduction of methylene blue using NaBH4. Russ J Phys Chem B 16:869–876. https://doi.org/10.1134/S1990793122050074

Pyrzynska K (2011) Carbon nanotubes as sorbents in the analysis of pesticides. Chemosphere 83:1407–1413. https://doi.org/10.1016/j.chemosphere.2011.01.057

Qi L, Zhang K, Qin W, Hu Y (2020) Highly efficient flow-through catalytic reduction of methylene blue using silver nanoparticles functionalized cotton. Chem Eng J 388:124252. https://doi.org/10.1016/j.cej.2020.124252

Ramesha GK, Vijaya Kumara A, Muralidhara HB, Sampath S (2011) Graphene and graphene oxide as effective adsorbents toward anionic and cationic dyes. J Colloid Interface Sci 361:270–277. https://doi.org/10.1016/j.jcis.2011.05.050

Rashidi HR, Sulaiman NMN, Hashim NA, Hassan CRC, Ramli MR (2015) Synthetic reactive dye wastewater treatment by using nano-membrane filtration. Desalin Water Treat 55:86–95. https://doi.org/10.1080/19443994.2014.912964

Sadhukhan S, Ghosh TK, Rana D, Roy I, Bhattacharyya A, Sarkar G, Chakraborty M, Chattopadhyay D (2016) Studies on synthesis of reduced graphene oxide (RGO) via green route and its electrical property. Mater Res Bull 79:41–51. https://doi.org/10.1016/j.materresbull.2016.02.039

Sadri Moghaddam S, Alavi Moghaddam MR, Arami M (2010) Coagulation/flocculation process for dye removal using sludge from water treatment plant: optimization through response surface methodology. J Hazard Mater 175:651–657. https://doi.org/10.1016/j.jhazmat.2009.10.058

Safari J, Gandomi-Ravandi S, Ashiri S (2016) Organosilane sulfonated graphene oxide in the Biginelli and Biginelli-like reactions. New J Chem 40:512–520. https://doi.org/10.1039/C5NJ01741F

Samadaei F, Salami-Kalajahi M, Roghani-Mamaqani H, Banaei M (2015) A structural study on ethylenediamine- and poly(amidoamine)-functionalized graphene oxide: simultaneous reduction, functionalization, and formation of 3D structure. RSC Adv 5:71835–71843. https://doi.org/10.1039/C5RA12086A

Sankaran A, Kumaraguru K, Balraj B (2021) Structural and optical behavior of CuO/Ag and CuO/Ag/Au nanocatalysts synthesized via a novel two step synthesis approach for enhancement of catalytic activity. J Inorg Organomet Polym Mater 31:151–161. https://doi.org/10.1007/s10904-020-01655-x

Tan J (2024) Ag nanoparticles functionalized melamine sponges for enhanced catalytic reduction of methylene blue. Chem Eng Sci 291:119963. https://doi.org/10.1016/j.ces.2024.119963

Tawade AK, Kamble BB, Sharma KKK, Tayade SN (2020) Simultaneous electrochemical investigations of dopamine and uric acid by in situ amino functionalized reduced grahene oxide. SN Appl Sci 2:1082. https://doi.org/10.1007/s42452-020-2806-0

Vijina C, Majitha KP, Damodaran SP (2023) Amine-functionalized reduced graphene oxide-supported silver nanoparticles for superior catalytic reduction of organic pollutants. Environ Sci Pollut Res 30:96114–96124. https://doi.org/10.1007/s11356-023-29115-2

Vinodh R, Babu CM, Abidov A, Palanichamy M, Jang HT (2019) Facile synthesis of amine modified silica/reduced graphene oxide composite sorbent for CO2 adsorption. Mater Lett 247:44–47. https://doi.org/10.1016/j.matlet.2019.03.082

Wadhwani SA, Shedbalkar UU, Nadhe S, Singh R, Chopade BA (2018) Decolorization of textile dyes by combination of gold nanocatalysts obtained from Acinetobacter sp. SW30 and NaBH4. Environ Technol Innov 9:186–197. https://doi.org/10.1016/j.eti.2017.12.001

Weremfo A, Abassah-Oppong S, Adulley F, Dabie K, Seidu-Larry S (2023) Response surface methodology as a tool to optimize the extraction of bioactive compounds from plant sources. J Sci Food Agric 103:26–36. https://doi.org/10.1002/jsfa.12121

Yang S-T, Chen S, Chang Y, Cao A, Liu Y, Wang H (2011) Removal of methylene blue from aqueous solution by graphene oxide. J Colloid Interface Sci 359:24–29. https://doi.org/10.1016/j.jcis.2011.02.064

Yardım Y, Vandeput M, Çelebi M, Şentürk Z, Kauffmann J-M (2017) A reduced graphene oxide-based electrochemical DNA biosensor for the detection of interaction between cisplatin and DNA based on guanine and adenine oxidation signals. Electroanalysis 29:1451–1458. https://doi.org/10.1002/elan.201600804

Yigit A, Pınar PT, Akinay Y, Alma MH, Menges N (2021) Nanotube-boramidic acid derivative for dopamine sensing. ChemistrySelect 6:6302–6313. https://doi.org/10.1002/slct.202101316

Yusuf M, Elfghi FM, Zaidi SA, Abdullah EC, Khan MA (2015) Applications of graphene and its derivatives as an adsorbent for heavy metal and dye removal: a systematic and comprehensive overview. RSC Adv 5:50392–50420. https://doi.org/10.1039/C5RA07223A